

Supplementary Table S2 (continued)

Gene Symbol	Description	Fold Change (log2)
Gnb4	guanine nucleotide binding protein (G protein), beta polypeptide 4	6.6
Col23a1	collagen, type XXIII, alpha 1	6.6
Atxn3	ataxin 3	6.6
RGD1563547	RGD1563547	6.6
Rhbdl1	rhomboid, veinlet-like 1 (<i>Drosophila</i>)	6.6
RGD1562726	similar to Putative protein C21orf62 homolog	6.5
Shank1	SH3 and multiple ankyrin repeat domains 1	6.5
Nln	neurolysin (metallopeptidase M3 family)	6.5
Epn3	epsin 3	6.5
Ccdc64	coiled-coil domain containing 64	6.5
Fam186b	family with sequence similarity 186, member B	6.5
Lyl1	lymphoblastic leukemia derived sequence 1	6.5
Rc3h2	ring finger and CCCH-type domains 2	6.4
Nexn	nexilin (F actin binding protein)	6.4
Map3k1	mitogen activated protein kinase kinase kinase 1	6.4
Akt1	v-akt murine thymoma viral oncogene homolog 1	6.4
Tmem171	transmembrane protein 171	6.4
Bpifb1	BPI fold containing family B, member 1	6.4
Tmtc4	transmembrane and tetratricopeptide repeat containing 4	6.4
Ormdl3	ORM1-like 3 (<i>S. cerevisiae</i>)	6.4
Olr1225	olfactory receptor 1225	6.3
Bcmo1	beta-carotene 15,15'-monooxygenase 1	6.3
Spink2	serine peptidase inhibitor, Kazal type 2 (acrosin-trypsin inhibitor)	6.3
Rassf5	Ras association (RalGDS/AF-6) domain family member 5	6.3
Map4k1	mitogen activated protein kinase kinase kinase kinase 1	6.3
Acads	acyl-CoA dehydrogenase, C-2 to C-3 short chain	6.3
Fcgbp	Fc fragment of IgG binding protein	6.3
Krt8	keratin 8	6.3
Mxd1	max dimerization protein 1	6.2
Cdca8	cell division cycle associated 8	6.2
Efna4	ephrin A4	6.2
Rbmx	RNA binding motif protein, X-linked	6.2
Pcdhb9	protocadherin beta 9	6.2
Fkbp11	FK506 binding protein 11	6.2
B3galt4	UDP-Gal:betaGlcNAc beta 1,3-galactosyltransferase, polypeptide 4	6.1
Ppp2r5c	protein phosphatase 2, regulatory subunit B', gamma	6.1
Lyst	lysosomal trafficking regulator	6.1
Zbtb40	zinc finger and BTB domain containing 40	6.1
Pa2g4	proliferation-associated 2G4	6.1
Zbtb8a	zinc finger and BTB domain containing 8a	6.1
Reep1	receptor accessory protein 1	6.1
Actn1	actinin, alpha 1	6.0
Ifih1	interferon induced with helicase C domain 1	6.0
Kctd11	potassium channel tetramerisation domain containing 11	6.0
Rin3	Ras and Rab interactor 3	6.0
Tasp1	taspase, threonine aspartase 1	6.0
Mef2d	myocyte enhancer factor 2D	6.0
Gpx2	glutathione peroxidase 2	6.0
Atp6v1e2	ATPase, H transporting, lysosomal V1 subunit E2	6.0
Usp12	ubiquitin specific peptidase 12	6.0

Gene expression in cartilage

Supplementary Table S2 (continued)

Gene Symbol	Description	Fold Change (log2)
Al13	alpha-1-inhibitor III	6.0
Clgn	calmegin	6.0
Smtn	smoothelin	6.0
Pde7b	phosphodiesterase 7B	5.9
Zbtb38	zinc finger and BTB domain containing 38	5.9
Arde2	arrestin domain containing 2	5.9
Lrcc27	leucine rich repeat containing 27	5.9
Rufy2	RUN and FYVE domain containing 2	5.9
Traf3ip1	TNF receptor-associated factor 3 interacting protein 1	5.9
Pex11a	peroxisomal biogenesis factor 11 alpha	5.9
Smpd3	sphingomyelin phosphodiesterase 3, neutral membrane	5.9
Esp11	extra spindle pole bodies homolog 1 (<i>S. cerevisiae</i>)	5.8
Rin1	Ras and Rab interactor-like	5.8
Fam198b	family with sequence similarity 198, member B	5.8
Slc30a1	solute carrier family 30 (zinc transporter), member 1	5.8
Abi3	ABI family, member 3	5.8
Ramp2	receptor (G protein-coupled) activity modifying protein 2	5.8
Exosc2	exosome component 2	5.8
Opn4	opsin 4	5.7
Atf3	activating transcription factor 3	5.7
Evc2	Ellis van Creveld syndrome 2 homolog (human)	5.7
Ang1	angiogenin, ribonuclease A family, member 1	5.7
Mfsd7	major facilitator superfamily domain containing 7	5.7
Lyzl6	lysozyme-like 6	5.7
Tbxa2r	thromboxane A2 receptor	5.7
Fam132a	family with sequence similarity 132, member A	5.7
LOC100362783	Uncharacterized protein C7orf61 homolog	5.7
Naalad11	N-acetylated alpha-linked acidic dipeptidase-like 1	5.7
Spa17	sperm autoantigenic protein 17	5.6
Exnef	exonuclease NEF-sp	5.6
Tpk1	thiamin pyrophosphokinase 1	5.6
LOC502684	hypothetical protein LOC502684	5.6
Kif20b	kinesin family member 20B	5.6
Clint1	clathrin interactor 1	5.6
Iah1	isoamyl acetate-hydrolyzing esterase 1 homolog (<i>S. cerevisiae</i>)	5.6
Slc39a12	solute carrier family 39 (zinc transporter), member 12	5.6
Epb49	erythrocyte membrane protein band 4.9 (dematin)	5.6
Ankrd34a	ankyrin repeat domain 34A	5.6
Aoc3	amine oxidase, copper containing 3 (vascular adhesion protein 1)	5.5
Ppp1r1a	protein phosphatase 1, regulatory (inhibitor) subunit 1A	5.5
Polb	polymerase (DNA directed), beta	5.5
Supt7l	suppressor of Ty 7 (<i>S. cerevisiae</i>)-like	5.5
Tg	thyroglobulin	5.5
Cd46	CD46 molecule, complement regulatory protein	5.5
Cntrob	centrobin, centrosomal BRCA2 interacting protein	5.5
Mepe	matrix extracellular phosphoglycoprotein	5.5
Lgals3bp	lectin, galactoside-binding, soluble, 3 binding protein	5.5
Smtnl2	smoothelin-like 2	5.4
Omd	osteomodulin	5.4
Pdhx	pyruvate dehydrogenase complex, component X	5.4

Supplementary Table S2 (continued)

Gene Symbol	Description	Fold Change (log2)
Rln1	relaxin 1	5.4
Rnf144a	ring finger protein 144A	5.4
Nod1	nucleotide-binding oligomerization domain containing 1	5.4
Heph	hephaestin	5.4
Usp31	ubiquitin specific peptidase 31	5.4
Dcps	decapping enzyme, scavenger	5.4
Stk35	serine/threonine kinase 35	5.3
Gbas	glioblastoma amplified sequence	5.3
Folr1	folate receptor 1 (adult)	5.3
Arfp1	ADP-ribosylation factor interacting protein 1	5.3
Slc16a1	solute carrier family 16, member 1	5.3
RGD1560909	similar to DNA segment, Chr 1, Brigham & Womens Genetics 0212 expressed	5.3
Lect1	leukocyte cell derived chemotaxin 1	5.3
Sbk1	SH3-binding domain kinase 1	5.3
LOC100360582	5',3'-nucleotidase, cytosolic	5.3
Ambp	alpha-1-microglobulin/bikunin precursor	5.3
Strpx	sushi-repeat-containing protein, X-linked	5.3
Tmem144	transmembrane protein 144	5.3
Zbtb3	zinc finger and BTB domain containing 3	5.3
Erp27	endoplasmic reticulum protein 27	5.3
Tgm1	transglutaminase 1, K polypeptide	5.2
Cdkn2aip	CDKN2A interacting protein	5.2
Megf9	multiple EGF-like-domains 9	5.2
Gdf10	growth differentiation factor 10	5.2
Rasa2	RAS protein activator like 2	5.2
Nme4	non-metastatic cells 4, protein expressed in	5.2
Fam83h	family with sequence similarity 83, member H	5.2
Ccdc86	coiled-coil domain containing 86	5.2
Prl8a5	prolactin family 8, subfamily a, member 5	5.2
Arnt	aryl hydrocarbon receptor nuclear translocator	5.2
Slc24a3	solute carrier family 24, member 3	5.1
Bhlhe22	basic helix-loop-helix family, member e22	5.1
Trim72	tripartite motif-containing 72	5.1
Ube2f	ubiquitin-conjugating enzyme E2F (putative)	5.1
Tmem151a	transmembrane protein 151A	5.1
Slc1a3	solute carrier family 1, member 3	5.1
Tff3	trefoil factor 3, intestinal	5.1
Mgrn1	mahogunin, ring finger 1	5.1
Slc7a5	solute carrier family 7, member 5	5.1
Spata2	spermatogenesis associated 2	5.0
Atg10	autophagy-related 10 (S. cerevisiae)	5.0
Pdzk1	PDZ domain containing 1	5.0
Rxra	retinoid X receptor alpha	5.0
Zfp94	zinc finger protein 94	5.0
Tmem209	transmembrane protein 209	5.0
Spopl	speckle-type POZ protein-like	5.0
B4galt1	UDP-Gal:betaGlcNAc beta 1,4- galactosyltransferase, polypeptide 1	5.0
Hmmr	hyaluronan mediated motility receptor (RHAMM)	5.0
Slc7a3	solute carrier family 7, member 3	4.9
Tpx2	TPX2, microtubule-associated, homolog (Xenopus laevis)	4.9

Supplementary Table S2 (continued)

Gene Symbol	Description	Fold Change (log2)
Serpinb8	serpin peptidase inhibitor, clade B (ovalbumin), member 8	4.9
Cpne5	copine V	4.9
Dnajc5	DnaJ (Hsp40) homolog, subfamily C, member 5	4.9
RGD1564482	RGD1564482	4.9
Chrne	cholinergic receptor, nicotinic, epsilon	4.9
Tifa	TRAF-interacting protein with forkhead-associated domain	4.9
Arhgap29	Rho GTPase activating protein 29	4.9
Fert2	fer (fms/fps related) protein kinase, testis specific 2	4.9
Max	MYC associated factor X	4.8
Fam122a	family with sequence similarity 122A	4.8
Cenpf	centromere protein F	4.8
Etv4	ets variant 4	4.8
Atp8b1	ATPase, Class I, type 8B, member 1	4.8
Cenl2	cyclin L2	4.8
Raly	RNA binding protein, autoantigenic	4.8
Dnajb4	DnaJ (Hsp40) homolog, subfamily B, member 4	4.8
Recql4	RecQ protein-like 4	4.8
Magt1	magnesium transporter 1	4.8
Nnat	neuronatin	4.8
Nkd1	naked cuticle homolog 1 (<i>Drosophila</i>)	4.8
Irak4	interleukin-1 receptor-associated kinase 4	4.8
Scn1a	sodium channel, voltage-gated, type I, alpha	4.8
Ptch1	patched 1	4.7
Case5	cancer susceptibility candidate 5	4.7
Adamts1	ADAM metallopeptidase with thrombospondin type 1 motif, 1	4.7
Kbtbd11	kelch repeat and BTB (POZ) domain containing 11	4.7
RGD1311863	similar to RIKEN cDNA 2410127L17	4.7
Ribe1	RIB43A domain with coiled-coils 1	4.7
Ghdc	GH3 domain containing	4.7
Hspa12a	heat shock protein 12A	4.7
Hsd12	hydroxysteroid dehydrogenase like 2	4.7
Rebtb2	RCC1 and BTB domain containing protein 2	4.7
Trmt11	tRNA methyltransferase 11 homolog (<i>S. cerevisiae</i>)	4.6
Myo10	myosin X	4.6
Ankrd6	ankyrin repeat domain 6	4.6
T2	brachyury 2	4.6
Zbtb10	zinc finger and BTB domain containing 10	4.6
Ftsjd1	FtsJ methyltransferase domain containing 1	4.6
Lgals4	lectin, galactoside-binding, soluble, 4	4.6
Galnt7	GalNAc-T7	4.6
Slc25a37	solute carrier family 25, member 37	4.6
Sstr1	somatostatin receptor 1	4.6
Gpm6b	glycoprotein m6b	4.6
Dcp1a	DCP1 decapping enzyme homolog A (<i>S. cerevisiae</i>)	4.6
Asz1	ankyrin repeat, SAM and basic leucine zipper domain containing 1	4.6
Tmem86a	transmembrane protein 86A	4.6
Ugt1a6	UDP glucuronosyltransferase 1 family, polypeptide A6	4.5
Prss36	protease, serine, 36	4.5
Tia1	Tia1 cytotoxic granule-associated RNA binding protein-like 1	4.5
Defb27	defensin beta 27	4.5

Supplementary Table S2 (continued)

Gene Symbol	Description	Fold Change (log2)
Tbkbp1	TBK1 binding protein 1	4.4
Fam176a	family with sequence similarity 176, member A	4.4
Mylk3	myosin light chain kinase 3	4.4
C1qtnf1	C1q and tumor necrosis factor related protein 1	4.4
Sbno2	strawberry notch homolog 2 (Drosophila)	4.4
Fsip1	fibrous sheath interacting protein 1	4.4
Chaf1b	chromatin assembly factor 1, subunit B (p60)	4.4
MGC95152	similar to B230212L03Rik protein	4.4
Wdr72	WD repeat domain 72	4.4
Polq	polymerase (DNA directed), theta	4.3
Ugt1a9	UDP glucuronosyltransferase 1 family, polypeptide A9	4.3
Mtf2	metal response element binding transcription factor 2	4.3
Wwox	WW domain-containing oxidoreductase	4.3
Ugt1a8	UDP glycosyltransferase 1 family, polypeptide A8	4.3
Ugt1a7c	UDP glucuronosyltransferase 1 family, polypeptide A7C	4.3
Ugt1a5	UDP glucuronosyltransferase 1 family, polypeptide A5	4.3
Ugt1a3	UDP glycosyltransferase 1 family, polypeptide A3	4.3
Ugt1a2	UDP glucuronosyltransferase 1 family, polypeptide A2	4.3
Ugt1a1	UDP glucuronosyltransferase 1 family, polypeptide A1	4.3
Sgms2	sphingomyelin synthase 2	4.3
Prkar2b	protein kinase, cAMP dependent regulatory, type II beta	4.3
Decr2	2,4-dienoyl CoA reductase 2, peroxisomal	4.3
Fam83d	family with sequence similarity 83, member D	4.3
Sult1a1	sulfotransferase family, cytosolic, 1A, phenol-preferring, member 1	4.3
Kifc1	kinesin family member C1	4.2
Opa1	optic atrophy 1 homolog (human)	4.2
Rab11fip2	RAB11 family interacting protein 2 (class I)	4.2
Gtse1	G-2 and S-phase expressed 1	4.2
Slc27a6	solute carrier family 27 (fatty acid transporter), member 6	4.2
Cep55	centrosomal protein 55	4.2
Agmo	alkylglycerol monooxygenase	4.2
Slc25a30	solute carrier family 25, member 30	4.2
Lcn2	lipocalin 2	4.2
Nalcn	sodium leak channel, non-selective	4.2
Robo2	roundabout homolog 2 (Drosophila)	4.2
Asrg1l	asparaginase like 1	4.2
Lepr	leptin receptor	4.2
Mbtps2	membrane-bound transcription factor peptidase, site 2	4.1
Plip	plasmolipin	4.1
Slc22a20	solute carrier family 22 (organic anion transporter), member 20	4.1
Extl3	exostoses (multiple)-like 3	4.1
Pygo1	pygopus 1	4.1
Lefty1	left right determination factor 1	4.1
Map4k2	mitogen activated protein kinase kinase kinase kinase 2	4.1
mf141	ring finger protein 141	4.1
Ocr1	oculocerebrorenal syndrome of Lowe	4.1
Mfap5	microfibrillar associated protein 5	4.1
Crk	v-crk sarcoma virus CT10 oncogene homolog (avian)	4.1
Cmtm8	CKLF-like MARVEL transmembrane domain containing 8	4.0
Ddx25	DEAD (Asp-Glu-Ala-Asp) box polypeptide 25	4.0

Gene expression in cartilage

Supplementary Table S2 (continued)

Gene Symbol	Description	Fold Change (log2)
Kcnh2	potassium voltage-gated channel, subfamily H (eag-related), member 2	4.0
Fndc3b	fibronectin type III domain containing 3B	4.0
Fxr1	fragile X mental retardation, autosomal homolog 1	4.0
Dkk1	dickkopf homolog 1 (<i>Xenopus laevis</i>)	4.0
Nphp3	nephronophthisis 3 (adolescent)	4.0
Srsf10	serine/arginine-rich splicing factor 10	4.0
Ttk2	tau tubulin kinase 2	4.0
Homez	homeobox and leucine zipper encoding	4.0
Stard5	StAR-related lipid transfer (START) domain containing 5	4.0
Cxadr	coxsackie virus and adenovirus receptor	4.0
Ano4	anoctamin 4	4.0
Slc6a2	solute carrier family 6, member 2	4.0
Ube2cbp	ubiquitin-conjugating enzyme E2C binding protein	4.0
Mitf	microphthalmia-associated transcription factor	3.9
Erc1	ELKS/RAB6-interacting/CAST family member 1	3.9
Pik3cd	phosphoinositide-3-kinase, catalytic, delta polypeptide	3.9
Tbc1d7	TBC1 domain family, member 7	3.9
Akr1e2	aldo-keto reductase family 1, member E2	3.9
Rab3d	RAB3D, member RAS oncogene family	3.9
Cenpm	centromere protein M	3.9
Chchd5	coiled-coil-helix-coiled-coil-helix domain containing 5	3.9
Prrx2	paired related homeobox 2	3.8
Slmo1	slowmo homolog 1 (<i>Drosophila</i>)	3.8
Eml2	echinoderm microtubule associated protein like 2	3.8
Sh3bp1	SH3-domain binding protein 1	3.8
Btrc	beta-transducin repeat containing	3.8
Phlpp1	PH domain and leucine rich repeat protein phosphatase 1	3.8
Rpp38	ribonuclease P/MRP 38 subunit (human)	3.8
Tnks	tankyrase, TRF1-interacting ankyrin-related ADP-ribose polymerase	3.8
Reep6	receptor accessory protein 6	3.8
Fblim1	filamin binding LIM protein 1	3.8
Fam25a	family with sequence similarity 25, member A	3.7
Sema4g	Semaphorin 4G	3.7
Ppp1r3a	protein phosphatase 1, regulatory subunit 3A	3.7
Traf3ip3	TRAF3 interacting protein 3	3.7
Rnf17	ring finger protein 17	3.7
Steap1	six transmembrane epithelial antigen of the prostate 1	3.7
Ikbip	IKBKB interacting protein	3.7
Mpp2	membrane protein, palmitoylated 2 (MAGUK p55 subfamily member 2)	3.7
Pde12	phosphodiesterase 12	3.7
Lxn	latexin	3.7
Alox12	arachidonate 12-lipoxygenase	3.7
Nt5c3	5'-nucleotidase, cytosolic III	3.6
Gnb5	guanine nucleotide binding protein (G protein), beta 5	3.6
Jph3	junctophilin 3	3.6
Ttc7b	tetratricopeptide repeat domain 7B	3.6
D2hgdh	D-2-hydroxyglutarate dehydrogenase	3.6
Cdkn2c	cyclin-dependent kinase inhibitor 2C (p18, inhibits CDK4)	3.6
Cachd1	cache domain containing 1	3.6
Kbtbd5	kelch repeat and BTB (POZ) domain containing 5	3.6

Supplementary Table S2 (continued)

Gene Symbol	Description	Fold Change (log2)
Pex7	peroxisomal biogenesis factor 7	3.6
Tomm34	translocase of outer mitochondrial membrane 34	3.6
Arse	arylsulfatase E (chondrodysplasia punctata 1)	3.6
Fubp1	far upstream element (FUSE) binding protein 1	3.6
RGD1563159	RGD1563159	3.6
Npw	neuropeptide W	3.6
Mia	melanoma inhibitory activity	3.6
Mcee	methylmalonyl CoA epimerase	3.5
RGD1563325	similar to hypothetical protein MGC17943	3.5
Slc26a4	solute carrier family 26, member 4	3.5
Fbxo28	F-box protein 28	3.5
Ccdc102a	coiled-coil domain containing 102A	3.5
Rtn4ip1	reticulon 4 interacting protein 1	3.5
Lrrc4	leucine rich repeat containing 4	3.5
RGD1305537	similar to RIKEN cDNA 3110001I22	3.5
Tprg1	tumor protein p63 regulated 1	3.5
Kenn2	potassium intermediate/small conductance calcium-activated channel, N2	3.5
Rgl3	ral guanine nucleotide dissociation stimulator-like 3	3.5
Sim2	single-minded homolog 2 (Drosophila)	3.5
Usp46	ubiquitin specific peptidase 46	3.5
Ehd3	EH-domain containing 3	3.5
Cubn	cubilin (intrinsic factor-cobalamin receptor)	3.4
Cers1	ceramide synthase 1	3.4
Gdf1	growth differentiation factor 1	3.4
Piwil2	piwi-like 2 (Drosophila)	3.4
Rabif	RAB interacting factor	3.4
Hyal3	hyaluronoglucosaminidase 3	3.4
Rab30	RAB30, member RAS oncogene family	3.4
Sytl1	synaptotagmin-like 1	3.4
Gpc2	glypican 2	3.4
Zmat4	zinc finger, matrin type 4	3.3
Ttc25	tetratricopeptide repeat domain 25	3.3
Il22	interleukin 22	3.3
Mid1ip1	MID1 interacting protein 1 (gastrulation specific G12 homolog (zebrafish))	3.3
Mutyh	mutY homolog (E. coli)	3.3
Flnc	filamin C, gamma	3.3
Tshz3	teashirt zinc finger homeobox 3	3.3
Pdpx	pyridoxal (pyridoxine, vitamin B6) phosphatase	3.3
Acsl3	acyl-CoA synthetase long-chain family member 3	3.3
Lpin1	lipin 1	3.2
Zc3hav1	zinc finger CCCH type, antiviral 1	3.2
Bfsp1	beaded filament structural protein 1	3.2
Fermt3	fermitin family member 3	3.2
Trim13	tripartite motif-containing 13	3.2
Magix	MAG1 family member, X-linked	3.2
Cyp2d4	cytochrome P450, family 2, subfamily d, polypeptide 4	3.2
Abcb7	ATP-binding cassette, subfamily B (MDR/TAP), member 7	3.2
Pigy	phosphatidylinositol glycan anchor biosynthesis, class Y	3.2
Ppm1h	protein phosphatase 1H (PP2C domain containing)	3.2
Tm7sf2	transmembrane 7 superfamily member 2	3.2

Gene expression in cartilage

Supplementary Table S2 (continued)

Gene Symbol	Description	Fold Change (log2)
Wnt3	wingless-type MMTV integration site family, member 3	3.2
Cp	ceruloplasmin	3.2
St5	suppression of tumorigenicity 5	3.2
Myo5a	myosin VA	3.1
Ptpla	protein tyrosine phosphatase-like (proline instead of catalytic arginine), member a	3.1
Smo	smoothened, frizzled family receptor	3.1
Nog	noggin	3.1
Mmp3	matrix metalloproteinase 3	3.1
Trim37	tripartite motif-containing 37	3.1
Lactb2	lactamase, beta 2	3.1
Slc5a12	solute carrier family 5 (sodium/glucose cotransporter), member 12	3.0
RGD1310553	similar to expressed sequence A1597479	3.0
Tmem38b	transmembrane protein 38B	3.0
Trim14	tripartite motif-containing 14	2.9
Spata1	spermatogenesis associated 1	2.9
RGD1561149	similar to mKIAA1522 protein	2.9
Tmem79	transmembrane protein 79	2.9
Ctnnd1	catenin (cadherin associated protein), delta 1	2.9
Dnaja4	DnaJ (Hsp40) homolog, subfamily A, member 4	2.9
Rhbdd2	rhomboid domain containing 2	2.9
Nudt21	nudix (nucleoside diphosphate linked moiety X)-type motif 21	2.9
Pdk3	pyruvate dehydrogenase kinase, isozyme 3	2.9
Arhgap4	Rho GTPase activating protein 4	2.9
Stk38l	serine/threonine kinase 38 like	2.9
Hsf4	heat shock transcription factor 4	2.9
Mark4	MAP/microtubule affinity-regulating kinase 4	2.9
Fto	fat mass and obesity associated	2.8
Vps72	vacuolar protein sorting 72 homolog (S. cerevisiae)	2.8
Pesk6	proprotein convertase subtilisin/kexin type 6	2.8
Ube2l6	ubiquitin-conjugating enzyme E2L 6	2.8
LOC361346	similar to chromosome 18 open reading frame 54	2.8
Mterfd1	MTERF domain containing 1	2.8
Gpn2	GPN-loop GTPase 2	2.8
LOC100362431	tetratricopeptide repeat domain 30B	2.8
Arsg	arylsulfatase G	2.8
RGD1308428	similar to RIKEN cDNA 4931406P16	2.8
Zfp655	zinc finger protein 655	2.7
Trhr	thyrotropin releasing hormone receptor	2.7
Ccdc61	coiled-coil domain containing 61	2.7
Azi1	5-azacytidine induced 1	2.7
Dnmt3b	DNA (cytosine-5-)-methyltransferase 3 beta	2.7
RGD1563941	similar to hypothetical protein FLJ20010	2.7
Nradd	neurotrophin receptor associated death domain	2.7
Mapk1ip11	mitogen-activated protein kinase 1 interacting protein 1-like	2.7
Col9a2	collagen, type IX, alpha 2	2.7
Col9a1	collagen, type IX, alpha 1	2.7
Spin1	spindlin 1	2.7
Cib2	calcium and integrin binding family member 2	2.7
C1qtnf3	C1q and tumor necrosis factor related protein 3	2.6
Epyc	epiphycan	2.6

Supplementary Table S2 (continued)

Gene Symbol	Description	Fold Change (log2)
Tmem169	transmembrane protein 169	2.6
Stradb	STE20-related kinase adaptor beta	2.6
Fkbp7	FK506 binding protein 7	2.6
Rps6ka1	ribosomal protein S6 kinase polypeptide 1	2.6
Tctex1d2	Tctex1 domain containing 2	2.6
Plekhh3	pleckstrin homology domain containing, family H (with MyTH4 domain) member 3	2.6
Gins4	GINS complex subunit 4 (Sld5 homolog)	2.6
Wdr19	WD repeat domain 19	2.6
Trub1	TruB pseudouridine (psi) synthase homolog 1 (E. coli)	2.6
Fahd1	fumarylacetoacetate hydrolase domain containing 1	2.6
Slc34a3	solute carrier family 34 (sodium phosphate), member 3	2.6
Edem3	ER degradation enhancer, mannosidase alpha-like 3	2.6
Slc12a3	solute carrier family 12 (sodium/chloride transporters), member 3	2.5
Cb1c	Cas-Br-M (murine) ecotropic retroviral transforming sequence c	2.5
LOC499643	similar to hypothetical protein FLJ25371	2.5
Mug2	murinoglobulin 2	2.5
Isg20	interferon stimulated exonuclease gene 20	2.5
Lum	lumican	2.5
Zpbp2	zona pellucida binding protein 2	2.5
Cpne8	copine VIII	2.5
Pir	pirin (iron-binding nuclear protein)	2.5
Zfp7	zinc finger protein 7	2.4
Pcsk1n	proprotein convertase subtilisin/kexin type 1 inhibitor	2.4
Sec23ip	SEC23 interacting protein	2.4
Rab4b	RAB4B, member RAS oncogene family	2.4
Tomm40	translocase of outer mitochondrial membrane 40 homolog (yeast)	2.4
Tapbp	TAP binding protein	2.4
Pi15	peptidase inhibitor 15	2.4
Hac11	2-hydroxyacyl-CoA lyase 1	2.4
Usp15	ubiquitin specific peptidase 15	2.4
G3bp2	GTPase activating protein (SH3 domain) binding protein 2	2.3
Zdhhc2	zinc finger, DHHC-type containing 2	2.3
Rhobtb3	Rho-related BTB domain containing 3	2.3
Fgd1	FYVE, RhoGEF and PH domain containing 1	2.3
Gpx7	glutathione peroxidase 7	2.3
RGD1305939	hypothetical LOC300074	2.3
Egfl7	EGF-like-domain, multiple 7	2.2
Slc3a1	solute carrier family 3, member 1	2.2
Man1a2	mannosidase, alpha, class 1A, member 2	2.2
Klhl36	kelch-like 36 (Drosophila)	2.2
Prrc1	proline-rich coiled-coil 1	2.2
Cep97	centrosomal protein 97	2.2
Anks1a	ankyrin repeat and sterile alpha motif domain containing 1A	2.2
Fam35a	family with sequence similarity 35, member A	2.2
Ece2	endothelin-converting enzyme 2	2.1
Slc8a3	solute carrier family 8 (sodium/calcium exchanger), member 3	2.1
Fbln5	fibulin 5	2.1
LOC690918	hypothetical protein LOC690918	2.0

Progression of ossification of the posterior longitudinal ligament of the thoracic spine following posterior decompression and stabilization

Clinical article

SHUREI SUGITA, M.D.,¹ HIROTAKE CHIKUDA, M.D., PH.D.,¹
KATSUSHI TAKESHITA, M.D., PH.D.,¹ ATSUSHI SEICHI, M.D., PH.D.,²
AND SAKAE TANAKA, M.D., PH.D.¹

¹Department of Orthopaedic Surgery, Faculty of Medicine, University of Tokyo, Tokyo; and ²Department of Orthopedics, Jichi Medical University, Tochigi, Japan

Object. Despite its potential clinical impact, information regarding progression of thoracic ossification of the posterior longitudinal ligament (OPLL) is scarce. Posterior decompression with stabilization is currently the primary surgical treatment for symptomatic thoracic OPLL; however, it remains unclear whether thoracic OPLL increases in size following spinal stabilization. It is also unknown whether patients' clinical symptoms worsen as OPLL size increases. In this retrospective case series study, the authors examined the postoperative progression of thoracic OPLL.

Methods. Nine consecutive patients with thoracic OPLL who underwent posterior decompression and fixation with a minimum follow-up of 3 years were included in this study. Thin-slice CT scans of the thoracic spine obtained at the time of surgery and the most recent follow-up were analyzed. The level of the most obvious protrusion of ossification was determined using the sagittal reconstructions, and the ossified area was measured on the axial reconstructed scan at the level of the most obvious protrusion of ossification using the DICOM (digital imaging and communications in medicine) software program. Myelopathy severity was assessed according to the Japanese Orthopaedic Association (JOA) scale score for lower-limb motor function on admission, at postoperative discharge, and at the last follow-up visit.

Results. The OPLL area was increased in all patients. The mean area of ossification increased from 83.6 ± 25.3 mm² at the time of surgery to 114.8 ± 32.4 mm² at the last follow-up visit. No patients exhibited any neurological deterioration due to OPLL progression.

Conclusions. The present study demonstrated that the size of the thoracic OPLL increased after spinal stabilization. Despite diminished local spinal motion, OPLL progression did not decrease or stop. Physicians should pay attention to ossification progression in patients with thoracic OPLL.

(<http://thejns.org/doi/abs/10.3171/2014.7.SPINE131191>)

KEY WORDS • posterior decompression and fixation • thoracic spine •
ossification of the posterior longitudinal ligament • progression

OSSIFICATION of the posterior longitudinal ligament (OPLL) is a condition of the spine characterized by the ectopic ossification of the spinal ligaments, potentially resulting in myelopathy due to spinal cord compression.¹¹ Although cervical OPLL progression is well documented in the literature,^{1,7,14,17,18} information regarding thoracic OPLL progression is lacking. Currently, posterior decompression and stabilization using instrumentation is a widely used first-choice treatment for symptomatic thoracic OPLL and achieves good short-

term outcomes.^{8,9,12,20} Anterior decompression is technically demanding, and the technique is associated with a high rate of complications.^{13,16} Spinal fixation with instrumentation is believed to diminish spinal cord damage and suppress further ossification by eliminating dynamic effects and reducing mechanical stress.¹⁹ Although the long-term progression of OPLL may compromise the surgical benefits, it remains unclear whether thoracic OPLL continues to grow after spinal stabilization. We hypothesized that spinal stabilization decreases the rate of OPLL progression by immobilizing the spine. To address this

Abbreviations used in this paper: JOA = Japanese Orthopaedic Association; OPLL = ossification of the posterior longitudinal ligament.

This article contains some figures that are displayed in color online but in black-and-white in the print edition.

issue, we examined thin-slice CT scans of patients with thoracic OPLL who underwent posterior decompression and fixation to examine the postoperative progression of thoracic OPLL.

Methods

Patients

There were 16 patients who underwent surgery for thoracic OPLL in the study period (from 2004 to 2007). Nine consecutive patients with thoracic OPLL who underwent posterior decompression and instrumentation-assisted fixation and had a minimum follow-up period of 3 years were included in this study. Three patients were excluded because they underwent OPLL extirpation via an anterior approach. Another 4 patients were excluded because the follow-up period was shorter than 3 years. All patients presented with progressive gait disturbance. We performed posterior decompression and fixation with a pedicle screw and rod system. The surgical plans were individualized according to OPLL extension and concomitant ossification of the ligamentum flavum. We fixed the spine 2–3 levels above and below the decompression levels and harvested local bone for grafting. In this group, plain radiography did not provide sufficient information regarding the instrumentation failure or ossification progression. Therefore, as part of the standard follow-up protocol, we obtained CT scans of OPLL patients every 2–3 years after surgery. We examined the thin-slice CT images of the thoracic spine obtained at the time of surgery and at the most recent follow-up visit. The CT scans were obtained with a slice thickness of 0.75 mm and a pixel size of 0.352×0.352 mm. The data were transferred via a DICOM (digital imaging and communications in medicine) network to a computer workstation using the OsiriX software program (OsiriX Imaging Software).⁵ Our institution's ethics board approved the study protocol.

Clinical Data

The patients' medical charts were reviewed for age, sex, type and extension of OPLL, and surgical procedure.

Myelopathy severity was assessed according to the Japanese Orthopaedic Association (JOA) scale for lower-limb motor function,⁸ which was administered on admission, at discharge, and the latest follow-up visit.

Measurement of Ossification

We reconstructed all preoperative CT scans for 3D multiplanar reconstruction and, using the sagittal reconstruction, determined the thoracic spine level with the most obvious level of ossification protrusion. We then measured the area of ossification on the axial reconstruction, which was set parallel to the endplate of the corresponding vertebra, using the OsiriX software program (Fig. 1). We also measured ossification area on the latest follow-up CT scan at the same level. All measurements were obtained twice for each CT data set by a board-certified spine surgeon (author S.S.), and the average value of the 2 measurements was used.

Statistical Analysis

We performed statistical analyses of the data using the Wilcoxon signed-rank test. Differences were considered statistically significant if *p* values were < 0.05 . Mean values are presented \pm SD.

Results

Demographic Data

The population included 3 males and 6 females, whose mean age was 56 ± 12.2 years (range 38–75 years). The mean follow-up period was 4.6 ± 2.0 years (range 3–9 years). The type of OPLL was continuous in 3 patients, mixed in 4 patients, and circumscribed in 2 patients. The level of OPLL, the level of the most obvious protrusion, and the surgical areas of decompression and fixation are shown in Table 1.

OPLL Progression

The area of OPLL was found to have increased in all patients (Table 2 and Fig. 2). The average area of ossification was 83.6 ± 25.3 mm² preoperatively and $114.8 \pm$

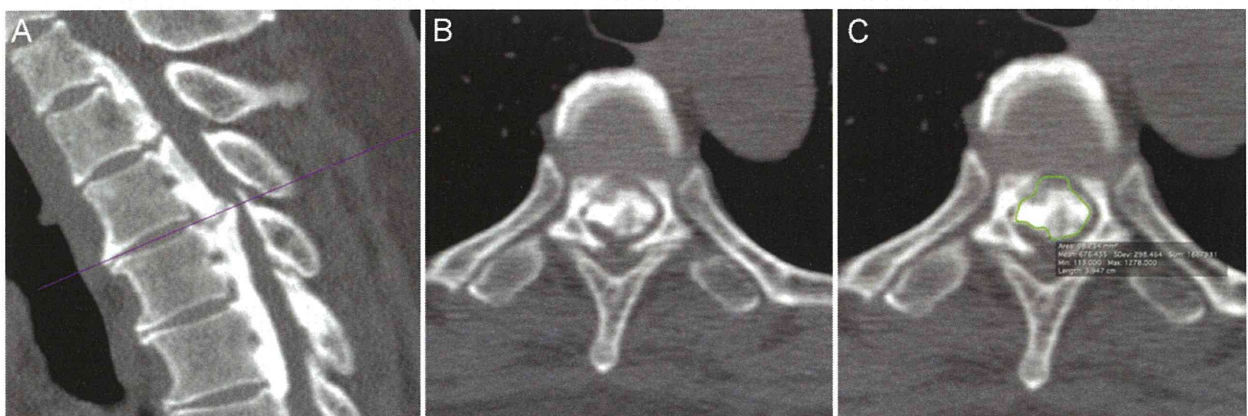


Fig. 1. **A:** The level of the most obvious protrusion of ossification was determined in the sagittal reconstruction (line). **B:** Cross-section at the determined level. **C:** The area of ossification, shown in green, was measured using a software function.

Postoperative progression of thoracic OPLL

TABLE 1: Patient demographics

Patient No.	Age (yrs), Sex	Type of OPLL	Extension of OPLL		Most Protruded OPLL Level	Surgical Level		Implant Density*	Rod Diameter (mm)	Follow-Up (yrs)
			Preop	Last Follow-Up		Decompression	Fixation			
1	48, M	mixed	C7-T10	C7-T10	T7-8	T1-10	T1-12	0.5	5.5	9
2	58, F	continuous	T3-6	T3-6	T5-6	T1-10	T1-10	0.55	5.5	3
3	38, M	circumscribed	T7-11	T7-11	T8-9	T7-L1	T5-L2	0.75	5.5	4
4	55, F	mixed	T4-10	T4-10	T5-6	T2-12	T2-12	0.55	6.5	3
5	64, F	continuous	T5-10	T3-L1	T7-8	T5-10	T5-10	0.92	5.5	7
6	39, M	circumscribed	T7-8	T7-8	T7-8	T5-10	T5-10	0.67	5.5	5
7	75, F	continuous	T3-9	T1-T11	T8-9	T5-10	T5-10	0.75	5.5	3
8	63, F	mixed	C4-T7	C4-T8	T3-4	C3-T8	C7-T8	0.56	6.5	4
9	70, F	mixed	C7-T5	C6-T5	T-2	C3-T6	C7-T8	0.67	5.5	3

* Implant density = no. implants per fixation segment \times 2.

32.4 mm² at the last follow-up visit. All areas of ossification increased in both width and thickness. Longitudinal OPLL progression was also noted in 4 of 9 patients. The rate of OPLL progression (the most recent size before surgery) was not correlated with the rod diameter or implant density. Neither screw loosening nor rod breakage was observed on any of the follow-up postoperative CT scans.

Clinical Course

The mean JOA score for lower-limb motor function was 1.8 ± 0.6 before surgery, 1.7 ± 0.6 at discharge, and 1.4 ± 0.7 at the most recent follow-up visit (Table 3). No patients exhibited neurological deterioration due to OPLL progression. One patient developed a severe gait disturbance due to an unrelated cause (worsening of lumbar canal stenosis), but the other 8 experienced gait disturbance improvements.

Illustrative Case

A 55-year-old woman presented with a walking disturbance and lower-extremity muscle weakness. She had mixed-type OPLL, extending from T-4 to T-10. The level

TABLE 2: Area of thoracic OPLL at the level of the most obvious protrusion

Patient No.	Area of the OPLL (mm ²)		Progression Rate (%)*
	Preop	At Last Follow-Up	
1	65.77	141.80	216
2	101.00	114.20	113
3	54.00	77.75	144
4	97.30	113.90	117
5	66.54	105.30	158
6	134.70	173.30	129
7	83.14	133.70	161
8	98.17	132.50	135
9	52.47	62.76	120

* The OPLL progression rate was determined by dividing the last follow-up area by the preoperative area.

of the most obvious protrusion was T5-6, with an OPLL area of 97.3 mm². We performed T2-10 laminectomy and posterior fixation from T-2 to T-12. Three years after surgery, the area of OPLL at T5-6 had increased to 113.9 mm² (Fig. 3).

Discussion

This is the first study to investigate the progression of thoracic OPLL after spinal stabilization. The use of thin-slice CT scans allowed us to conduct a detailed analysis of thoracic OPLL, which is difficult to do with plain radiographs. We found that the postoperative area of ossification increased both axially and longitudinally.

It is well recognized that cervical OPLL is progressive during the natural course of the disease and after decompressive surgery.^{4-6,10,15} Several investigators have reported that ossification progression aggravates myelopathy, whereas others have found no relationship between neurological function deterioration and ossification progression.^{2,5,7} This study is the first to show that ossification also progresses in the thoracic spine; however, this progression did not aggravate patients' myelopathy in the present series.

The pathomechanisms underlying the progression of OPLL remain unclear, but mechanical stress has been implicated as an exacerbating factor.¹⁹ Our initial hypothesis was that spinal stabilization suppresses OPLL progression by eliminating local motion of the spine. Contrary to our hypothesis, we found that OPLL continued to progress after spinal stabilization. A study with a longer follow-up period may provide additional information regarding the time course of OPLL progression.

There are several limitations associated with this study that deserve mention. First, the number of patients examined in this study was small. However, our findings were consistent among the cohort. Similarly, the length of follow-up was relatively short. Although OPLL progression did not result in functional deterioration in the present study, such progression could manifest in neurological dysfunction over a longer time span. Finally, we did not measure local spinal motion. A previous study showed that dynamic factors, such as the segmental range of mo-

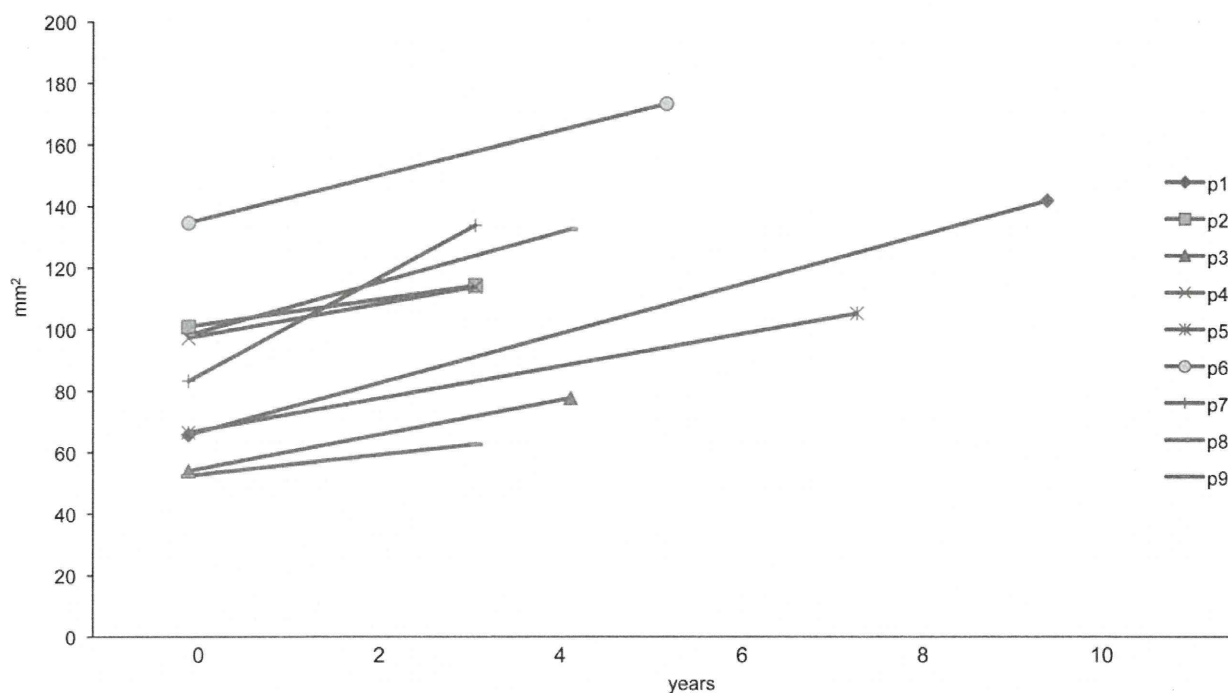


Fig. 2. Progression of OPLL during the follow-up period. The area of ossification increased in all patients. p = patient.

tion, contribute to the development of myelopathy in the cervical spine among patients with OPLL.³ However, it is difficult to precisely measure local thoracic spine motion with plain radiographs. Notably, we observed neither screw loosening nor rod breakage on any of the follow-up

CT scans, indicating that we successfully stabilized the patients' spines. A detailed analysis of spinal motion is needed in future studies.

Conclusions

The present study demonstrated that thoracic OPLL does not decrease or stop and affects a larger area over time, even after spinal stabilization. Although OPLL progression did not result in functional deterioration in this study, physicians should pay attention to continued ossification in patients with thoracic OPLL.

Disclosure

The authors report no conflict of interest concerning the mate-

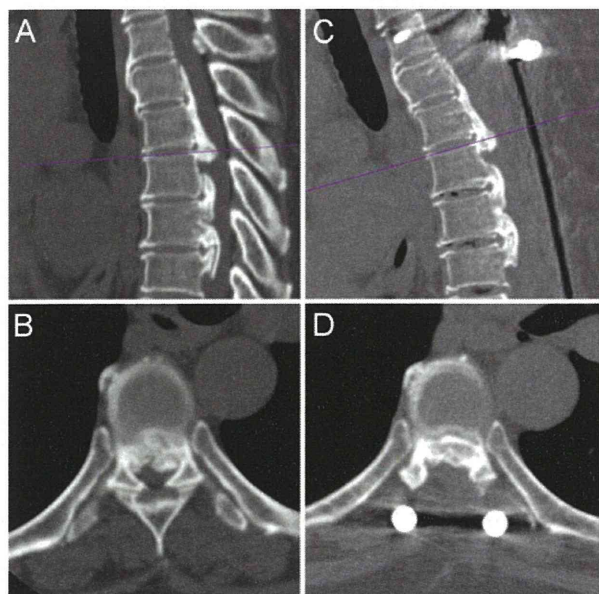


Fig. 3. A: The level of the most obvious protrusion of ossification was determined as previously described (line). B: Preoperative axial view of ossification at the determined level. C: The same level was selected on postoperative CT scans. D: Axial postoperative CT scan showing enlargement of the area of ossification.

TABLE 3: JOA scores for lower-limb motor function in each patient

Patient No.	JOA Score		
	Preop	Postop	Last Follow-Up
1	3	3	2
2	2	2	1
3	2	2	2
4	2	2	2
5	1	1	1
6	2	2	2
7	1	1	0
8	1	1	1
9	2	2	2

Postoperative progression of thoracic OPLL

rials or methods used in this study or the findings specified in this paper. This study was funded by a grant from the Ministry of Health, Labour, and Welfare of Japan (Research on Intractable Diseases grant no. H23-Nanchi-032). The funders played no role in the design of the study, data collection and analysis, decision to publish, or preparation of the manuscript.

Author contributions to the study and manuscript preparation include the following. Conception and design: Sugita, Chikuda. Acquisition of data: Sugita. Analysis and interpretation of data: Sugita. Drafting the article: Sugita. Critically revising the article: all authors. Reviewed submitted version of manuscript: all authors. Approved the final version of the manuscript on behalf of all authors: Sugita.

References

1. Fargen KM, Cox JB, Hoh DJ: Does ossification of the posterior longitudinal ligament progress after laminoplasty? Radiographic and clinical evidence of ossification of the posterior longitudinal ligament lesion growth and the risk factors for late neurologic deterioration. A review. **J Neurosurg Spine** 17:512–524, 2012
2. Fujimura Y, Nishi Y, Chiba K, Nakamura M, Hirabayashi K: Multiple regression analysis of the factors influencing the results of expansive open-door laminoplasty for cervical myelopathy due to ossification of the posterior longitudinal ligament. **Arch Orthop Trauma Surg** 117:471–474, 1998
3. Fujiyoshi T, Yamazaki M, Okawa A, Kawabe J, Hayashi K, Endo T, et al: Static versus dynamic factors for the development of myelopathy in patients with cervical ossification of the posterior longitudinal ligament. **J Clin Neurosci** 17:320–324, 2010
4. Inoue H, Ohmori K, Ishida Y, Suzuki K, Takatsu T: Long-term follow-up review of suspension laminotomy for cervical compression myelopathy. **J Neurosurg** 85:817–823, 1996
5. Iwasaki M, Kawaguchi Y, Kimura T, Yonenobu K: Long-term results of expansive laminoplasty for ossification of the posterior longitudinal ligament of the cervical spine: more than 10 years follow up. **J Neurosurg** 96 (2 Suppl):180–189, 2002
6. Kato Y, Iwasaki M, Fuji T, Yonenobu K, Ochi T: Long-term follow-up results of laminectomy for cervical myelopathy caused by ossification of the posterior longitudinal ligament. **J Neurosurg** 89:217–223, 1998
7. Kawaguchi Y, Kanamori M, Ishihara H, Nakamura H, Sugimori K, Tsuji H, et al: Progression of ossification of the posterior longitudinal ligament following en bloc cervical laminoplasty. **J Bone Joint Surg Am** 83-A:1798–1802, 2001
8. Kawahara N, Tomita K, Murakami H, Hato T, Demura S, Sekino Y, et al: Circumspinal decompression with dekyphosis stabilization for thoracic myelopathy due to ossification of the posterior longitudinal ligament. **Spine (Phila Pa 1976)** 33:39–46, 2008
9. Matsumoto M, Toyama Y, Chikuda H, Takeshita K, Kato T, Shindo S, et al: Outcomes of fusion surgery for ossification of the posterior longitudinal ligament of the thoracic spine: a multicenter retrospective survey. Clinical article. **J Neurosurg Spine** 15:380–385, 2011
10. Matsunaga S, Kukita M, Hayashi K, Shinkura R, Koriyama C, Sakou T, et al: Pathogenesis of myelopathy in patients with ossification of the posterior longitudinal ligament. **J Neurosurg** 96 (2 Suppl):168–172, 2002
11. Matsunaga S, Sakou T: Ossification of the posterior longitudinal ligament of the cervical spine: etiology and natural history. **Spine (Phila Pa 1976)** 37:E309–E314, 2012
12. Matsuyama Y, Sakai Y, Katayama Y, Imagama S, Ito Z, Wakao N, et al: Indirect posterior decompression with corrective fusion for ossification of the posterior longitudinal ligament of the thoracic spine: is it possible to predict the surgical results? **Eur Spine J** 18:943–948, 2009
13. Min JH, Jang JS, Lee SH: Clinical results of ossification of the posterior longitudinal ligament (OPLL) of the thoracic spine treated by anterior decompression. **J Spinal Disord Tech** 21:116–119, 2008
14. Murakami M, Seichi A, Chikuda H, Takeshita K, Nakamura K, Kimura A: Long-term follow-up of the progression of ossification of the posterior longitudinal ligament. Case report. **J Neurosurg Spine** 12:577–579, 2010
15. Ogawa Y, Toyama Y, Chiba K, Matsumoto M, Nakamura M, Takaishi H, et al: Long-term results of expansive open-door laminoplasty for ossification of the posterior longitudinal ligament of the cervical spine. **J Neurosurg Spine** 1:168–174, 2004
16. Ohtsuka K, Terayama K, Tsuchiya T, Wada K, Furukawa K, Ohkubo M: [A surgical procedure of the anterior decompression of the thoracic spinal cord through the posterior approach.] **Orthop Surg Traumatol** 26:1083–1090, 1983 (Jpn)
17. Seichi A, Hoshino Y, Ohnishi I, Kurokawa T: The role of calcium metabolism abnormalities in the development of ossification of the posterior longitudinal ligament of the cervical spine. **Spine (Phila Pa 1976)** 17 (3 Suppl):S30–S32, 1992
18. Suzuki K, Ishida Y, Ohmori K: Long term follow-up of diffuse idiopathic skeletal hyperostosis in the cervical spine. Analysis of progression of ossification. **Neuroradiology** 33:427–431, 1991
19. Tsukamoto N, Maeda T, Miura H, Jingushi S, Hosokawa A, Harimaya K, et al: Repetitive tensile stress to rat caudal vertebrae inducing cartilage formation in the spinal ligaments: a possible role of mechanical stress in the development of ossification of the spinal ligaments. **J Neurosurg Spine** 5:234–242, 2006
20. Yamazaki M, Mochizuki M, Ikeda Y, Sodeyama T, Okawa A, Koda M, et al: Clinical results of surgery for thoracic myelopathy caused by ossification of the posterior longitudinal ligament: operative indication of posterior decompression with instrumented fusion. **Spine (Phila Pa 1976)** 31:1452–1460, 2006

Manuscript submitted December 26, 2013.

Accepted July 7, 2014.

Please include this information when citing this paper: published online August 15, 2014; DOI: 10.3171/2014.7.SPINE131191.

Address correspondence to: Shurei Sugita, M.D., 7-3-1, Hongo, Bunkyo-ku, Tokyo 113-8655, Japan. email: ssugita-ky@umin.ac.jp.



Mead acid (20:3n-9) and n-3 polyunsaturated fatty acids are not associated with risk of posterior longitudinal ligament ossification: Results of a case-control study

Kei Hamazaki^{a,*}, Yoshiharu Kawaguchi^b, Masato Nakano^b, Taketoshi Yasuda^a, Shoji Seki^b, Takeshi Hori^b, Tomohito Hamazaki^c, Tomoatsu Kimura^b

^a Department of Public Health, Faculty of Medicine, University of Toyama, Toyama, Japan

^b Department of Orthopaedic Surgery, Faculty of Medicine, University of Toyama, Toyama, Japan

^c Toyama Jounan Daini Hospital, Toyama, Japan

ARTICLE INFO

Article history:

Received 19 November 2014

Received in revised form

26 December 2014

Accepted 8 January 2015

Keywords:

Ossification of the posterior longitudinal ligament

Case-control study

Mead acid

N-3 polyunsaturated fatty acids

ABSTRACT

Ossification of the posterior longitudinal ligament (OPLL) involves the replacement of ligamentous tissue with ectopic bone. Although genetics and heritability appear to be involved in the development of OPLL, its pathogenesis remains to be elucidated. Given previous findings that 5,8,11-eicosatrienoic acid [20:3n-9, Mead acid (MA)] has depressive effects on osteoblastic activity and anti-angiogenic effects, and that n-3 polyunsaturated fatty acids (PUFAs) have a preventive effect on heterotopic ossification, we hypothesized that both fatty acids would be involved in OPLL development. To examine the biological significance of these and other fatty acids in OPLL, we conducted this case-control study involving 106 patients with cervical OPLL and 109 age matched controls. Fatty acid composition was determined from plasma samples by gas chromatography. Associations between fatty acid levels and incident OPLL were evaluated by logistic regression. Contrary to our expectations, we found no significant differences between patients and controls in the levels of MA or n-3 PUFAs (e.g., eicosapentaenoic acid and docosahexaenoic acid). Logistic regression analysis did not reveal any associations with OPLL risk for MA or n-3 PUFAs. In conclusion, no potential role was found for MA or n-3 PUFAs in ectopic bone formation in the spinal canal.

© 2015 Elsevier Ltd. All rights reserved.

1. Introduction

Intraspinous canal ossification (ICO) is characterized by the replacement of ligamentous tissue with ectopic bone. ICO, such as ossification of the posterior longitudinal ligament (OPLL), often narrows the spinal canal and can cause cervical and thoracic myelopathy [1]. Asian populations were previously thought to show a predilection for this disease [2], but a number of cases have since been reported in Caucasian populations [3,4]. The pathogenesis of OPLL is not completely clear, although it may include a genetic background for systemic ossification [5].

Abbreviations: BMI, body mass index; CI, confidence interval; CT, computed tomography; EFA, essential fatty acid; ICO, intraspinal canal ossification; MA, Mead acid; OR, odds ratio; OPLL, ossification of the posterior longitudinal ligament; PGE₂, prostaglandin E₂; PUFA, polyunsaturated fatty acid

* Correspondence to: Department of Public Health, Faculty of Medicine, University of Toyama 2630 Sugitani, Toyama City, Toyama 9300194, Japan
Tel.: +81 76 434 7279; fax: +81 76 434 5023.

E-mail address: keihama@med.u-toyama.ac.jp (K. Hamazaki).

<http://dx.doi.org/10.1016/j.plefa.2015.01.003>

0952-3278/© 2015 Elsevier Ltd. All rights reserved.

Mead acid was discovered by Mead et al [6] as a fatty acid accumulated in fat-deficient rats. Measuring the fatty acid composition of various tissues of young chickens, fetal calves, and newborn pigs, Adkisson et al. [7] found unusually high levels of MA in cartilage. In particular, articular hyaline cartilage, which does not undergo calcification under normal conditions, had an MA level > 3-fold that of growth plate cartilage, which is eventually extensively calcified, whereas serum and cortical bone had negligibly low levels. Because cartilage lacks blood vessels and is composed of a highly charged extracellular matrix, essential fatty acids (EFAs) may not easily reach cartilaginous cells [7]; this is probably the main reason underlying the increased synthesis of MA in cartilage tissue, because MA increases only under conditions of EFA deficiency. Considering such findings, we previously explored the physiological effects of MA on osteoblasts and osteoclasts and found that MA reduced osteoblastic activity without affecting osteoclastic activity [8]. Furthermore, targeting the essential process of angiogenesis in heterotopic ossification [9], we previously found that MA also inhibits angiogenesis [10].

Prostaglandin E₂ (PGE₂) acts directly on osteoblasts, affecting osteogenesis by increasing DNA and collagen synthesis [11]. Ishida et al cultured spinal ligament from OPLL patients and found a PGE₂-

stimulated increase in adenosine-3',5'-cyclic monophosphate, indicating induction of osteoblastogenesis [12]. Wang et al hypothesized that heterotopic ossification could be prevented through anti-inflammatory effects by lowering the dietary n-6/n-3 polyunsaturated fatty acid ratio [13]; in the mechanism they propose, lowering the ratio would not only reduce the substrate of cyclooxygenase, but also partially inhibit cyclooxygenase expression and activity, thereby inhibiting PGE₂ synthesis and exerting a preventive effect [13].

Against this background, we hypothesized that both MA and n-3 PUFAs would be involved in OPLL development. To test this hypothesis and investigate their biological significance, in this study we evaluated the plasma concentrations of these and other fatty acids in patients with OPLL and controls.

2. Patients and methods

2.1. Subjects

All patients with OPLL and controls were recruited from the Department of Orthopaedic Surgery at Toyama University Hospital, Japan. Informed consent was obtained from all participants, and the study protocol was approved by the Ethics Committee of University of Toyama. The diagnosis of OPLL was based on radiological findings, including radiographs and computed tomography (CT) scans of the cervical, thoracic, and lumbar spine. Ankylosing spondylitis and metabolic diseases associated with OPLL, such as hypophosphatemic rickets/osteomalacia and hyperparathyroidism, were excluded by radiographic and biochemical examinations. The controls were age-matched patients with a diagnosis of cervical spondylosis and/or lumbar disc disease. None of the controls had ICO, as confirmed by CT.

2.2. Sampling and fatty acid analysis

Plasma samples were obtained from EDTA-anticoagulated blood and stored at -80 °C until analysis. Fatty acid composition of the total phospholipid fractions of plasma was determined. Total lipids were extracted according to the method of Bligh and Dyer [14]. The total phospholipid fraction was separated by thin-layer chromatography. For an internal standard, 1, 2-diheptadecanoyl-sn-glycero-3-phosphocholine (Avanti Polar Lipids, Inc., Alabaster, AL) was added. Total phospholipid fractions were subjected to transmethylation with methanolic hydrochloric acid, and the fatty acid composition was then analyzed by a gas chromatography system (GC-2014; Shimadzu Corporation, Kyoto, Japan) equipped with a capillary column DB-225 (length 30 m; internal diameter 0.25 mm; film 0.25 μm; J&M Scientific, Folsom, CA). The whole system was controlled by gas chromatography software (GC-Solution; Shimadzu Corporation). Values of fatty acids are expressed as area percentage of total fatty acids.

2.3. Statistical analysis

Data are expressed as means ± SD unless described otherwise. In descriptive analyses, differences in categorical and continuous variables among cases and controls were tested with the chi-square test and *t*-test, respectively. We used logistic regression to estimate odds ratios (ORs) for OPLL with a one-SD increase in each fatty acid levels (SD for each fatty acid was calculated from the controls) and adjusted for the following potential confounders: sex, age, body mass index (BMI, kg/m²), smoking (current smoker or not), alcohol consumption (never or seldom, occasionally, or frequent), and history of thyroid disease, renal dysfunction, or diabetes mellitus. To estimate the risk for OPLL for each plasma fatty acid level, we categorized the participants according to the quartile distributions of fatty acid levels in controls. We then performed logistic regression analysis to calculate ORs and 95% confidence intervals (CIs). Tests for trend involved assigning categorical numbers in their fatty acid quartile and evaluating this as a continuous variable. Correlations between each fatty acid level and BMI were calculated with simple regression analysis. The case and control samples had 32 and 22 missing values for smoking status and 32 and 20 for alcohol consumption, respectively. For these missing data, we added an extra category for the variable indicating missingness for imputation. Correspondingly, there were 13 and 16 missing values for weight and 11 and 15 for height. For these variables, we replaced each missing value with the mean control value. These imputations were only used for adjustment in regression analysis. Two-sided *p*-Values less than 0.05 were considered to indicate statistical significance. Data were analyzed using statistical software, SPSS, version 19.0 (IBM Japan, Tokyo).

3. Results

Baseline characteristics are shown in Table 1. No significant differences were seen between two groups in age, sex, BMI, number of subjects with obesity, or smoking status. However, significantly fewer OPLL patients consumed alcohol occasionally. No significant differences were found in the numbers of subjects with a history of thyroid disease, renal dysfunction, or diabetes. Comparison of the plasma fatty acid composition is shown in Table 2. OPLL patients were more likely to have higher levels of myristic acid, palmitic acid, and total saturated fatty acid than controls. There were no significant differences in MA and n-3 PUFA levels between the two groups. A subanalysis showed that male OPLL patients had significantly higher levels of myristic acid than male controls (0.28 ± 0.06 vs. 0.25 ± 0.06 , $p=0.021$), but no significant difference was found in women (data not shown). However, for palmitic acid, female OPLL patients had significant higher levels than female controls (29.4 ± 1.33 vs. 28.7 ± 1.53 , $p=0.016$), but no significant difference was found in men (data not shown).

Table 3 shows univariate and multivariate ORs for OPLL with a one-SD increase in each fatty acid level. No significant associations

Table 1
Patient demographics and baseline characteristics.

	Cases (n = 106)	Controls (n = 109)	<i>p</i> -Value*
Age, years	68 ± 10	69 ± 11	0.44
Male/female	65 / 41	60 / 49	0.35
BMI	24.8 ± 4.0	24.2 ± 3.8	0.46
Obesity (BMI ≥ 25) (%)	41 (38.7)	38 (34.9)	0.56
Smoking (never/current/ex)	48 / 14 / 12	57 / 11 / 19	0.43
Alcohol (never or seldom/occasionally/frequently)	41 / 7 / 26	43 / 23 / 23	0.02
Thyroid disease, n (%)	9 (8.5)	10 (9.2)	0.86
Renal dysfunction, n (%)	4 (3.8)	3 (2.8)	0.67
Diabetes, n (%)	28 (26.4)	21 (19.3)	0.21

BMI: body mass index

* Chi-square test for categorical variables and *t*-test for continuous variables.

Table 2
Baseline plasma fatty acid levels in cases and controls.

		Percentage of total fatty acids		
		Cases (n=106)	Controls (n=109)	p-Value
Saturated fatty acids				
Myristic acid	14:0	0.28 ± 0.08	0.26 ± 0.06	0.009
Palmitic acid	16:0	29.69 ± 1.37	29.10 ± 1.55	0.003
Stearic acid	18:0	14.30 ± 1.12	14.29 ± 1.09	0.95
Arachidic acid	20:0	0.41 ± 0.08	0.41 ± 0.08	0.76
Behenic acid	22:0	1.02 ± 0.24	0.99 ± 0.21	0.38
Lignoceric acid	24:0	0.96 ± 0.21	0.94 ± 0.19	0.46
Total		46.65 ± 1.22	45.98 ± 1.28	0.0001
Monounsaturated fatty acids				
Palmitoleic acid	16:1 n-7	0.55 ± 0.24	0.50 ± 0.21	0.12
Vaccenic acid	18:1 n-7	1.62 ± 0.29	1.66 ± 0.28	0.35
Oleic acid	18:1 n-9	9.18 ± 1.38	9.17 ± 1.41	0.98
Gondoic acid	20:1 n-9	0.17 ± 0.05	0.18 ± 0.07	0.23
Nervonic acid	24:1 n-9	2.04 ± 0.51	2.09 ± 0.55	0.42
Total		13.65 ± 1.62	13.70 ± 1.51	0.83
n-6 polyunsaturated fatty acids				
Linoleic acid	18:2 n-6	17.60 ± 3.29	17.74 ± 3.11	0.76
Eicosadienoic acid	20:2 n-6	0.32 ± 0.06	0.31 ± 0.05	0.64
Dihomo- γ -Linolenic acid	20:3 n-6	2.27 ± 0.67	2.22 ± 0.66	0.56
Arachidonic acid	20:4 n-6	8.22 ± 1.46	8.40 ± 1.50	0.39
Total		28.41 ± 3.30	28.66 ± 3.51	0.59
n-3 polyunsaturated fatty acids				
α -Linolenic acid	18:3 n-3	0.23 ± 0.07	0.23 ± 0.08	0.60
Eicosapentaenoic acid	20:5 n-3	2.82 ± 1.54	2.98 ± 1.77	0.46
Docosapentaenoic acid	22:5 n-3	1.15 ± 0.38	1.14 ± 0.30	0.86
Docosahexaenoic acid	22:6 n-3	7.10 ± 1.52	7.30 ± 1.44	0.32
Total		11.29 ± 2.79	11.66 ± 2.91	0.35
n-9 polyunsaturated fatty acid				
Mead acid	20:3 n-9	0.10 ± 0.09	0.09 ± 0.06	0.60
n-6/n-3 ratio				
		2.73 ± 0.93	2.68 ± 0.93	0.70

Values are means \pm SD.

were found between OPLL and MA or any n-3 PUFAs. Only total saturated fatty acids were positively associated with OPLL, and palmitic and myristic acid showed a tendency toward positive associations; however, a subanalysis revealed they had no significant association with OPLL in either men or women (data not shown). Table 4 shows crude and multivariable ORs for OPLL and 95% CIs according to the quartiles for some fatty acids. Table 4 presents only those fatty acids that showed marginal significance in Table 3, and MA, docosahexaenoic acid, and eicosapentaenoic acid regardless of significance. Palmitic acid was the only fatty acid in the multivariable models that showed a significant OR in the highest quartile compared with the lowest quartile. The trend test for palmitic acid was also significant. However, additional adjustment for 6 other confounding factors (obesity, smoking status, alcohol consumption, thyroid disease, renal dysfunction, and diabetes) showed only marginal significance (OR: 1.75, 95% CI: 0.90-3.39, $p=0.100$). In a subanalysis, ORs in the highest quartile for palmitic acid in a multivariable model (adjusted for sex and age) compared with the lowest quartile was not significant in men or women (data not shown).

4. Discussion

The relationship between fatty acid levels and risk for OPLL is reported here for the first time. Contrary to our expectations, we did

not find any significant differences in levels of MA or n-3 PUFAs between cases and controls. However, OPLL patients did have significantly higher levels of saturated fatty acids such as myristic acid and palmitic acid. Logistic regression analysis identified only palmitic acid, with a tendency toward a positive association with OPLL risk.

We recently demonstrated that MA significantly suppressed osteoblastic activity in vitro [8] and previously that MA has anti-angiogenic effects [10], which could confer some preventive effects against heterotopic ossification because angiogenesis is critical to bone formation [9]. However, contrary to our expectations, we found no association between MA and OPLL. This might be because we measured only plasma levels. Future studies should examine whether associations are present for samples taken from elsewhere in the spine, such as in the cerebrospinal fluid or ligament itself.

No association was found between lower n-3 PUFAs levels and a risk of OPLL, either. One of the reasons for this might be the plateau level (ceiling effect) of these fatty acids. Our previous epidemiological study showed that age is positively correlated with the blood n-3 PUFA levels [15], with old Japanese people showing plateau levels of n-3 PUFAs. Participants of the present study were generally elderly people (Table 1). Future studies should investigate a wider age range.

It is not clear why palmitic acid was significantly higher in OPLL patients than in controls and showed a tendency toward a positive association with OPLL risk. Interestingly, BMI was positively associated with palmitic acid ($r=0.18$, $p=0.006$), which is

Table 3

Results of univariate and multivariate analysis for OPLL according to a 1-SD increase in each fatty acid level, for 106 cases and 109 controls.

		Univariate	Multivariate ^a	Multivariate ^b
Saturated fatty acids				
Myristic acid	14:0	1.14 (0.99–1.30) [†]	1.15 (1.01–1.32)*	1.14 (0.99–1.32) [†]
Palmitic acid	16:0	1.24 (1.01–1.53)*	1.26 (1.01–1.56)*	1.22 (0.97–1.54) [†]
Stearic acid	18:0	1.00	1.00	1.02
Arachidic acid	20:0	0.98	0.99	0.98
Behenic acid	22:0	1.06	1.07	1.04
Lignoceric acid	24:0	1.05	1.05	1.04
Total		1.31 (1.08–1.59)**	1.30 (1.07–1.58)**	1.24 (1.02–1.52)*
Monounsaturated				
Palmitoleic acid	16:1 n-7	1.10	1.11	1.07
Vaccenic acid	18:1 n-7	0.94	0.94	0.94
Oleic acid	18:1 n-9	1.00	0.99	0.97
Gondoic acid	20:1 n-9	0.89	0.89	0.94
Nervonic acid	24:1 n-9	0.94	0.96	0.97
Total		0.99	0.99	0.96
n-6 polyunsaturated fatty acids				
Linoleic acid	18:2 n-6	0.98	0.97	0.99
Eicosadienoic acid	20:2 n-6	1.03	1.03	1.01
Dihomo- γ -Linolenic acid	20:3 n-6	1.04	1.04	1.04
Arachidonic acid	20:4 n-6	0.94	0.94	0.95
Total		0.96	0.95	0.98
n-3 polyunsaturated fatty acids				
α -Linolenic acid	18:3 n-3	0.96	0.97	0.98
Eicosapentaenoic acid	20:5 n-3	0.94	0.94	0.94
Docosapentaenoic acid	22:5 n-3	1.01	1.02	0.99
Docosahexaenoic acid	22:6 n-3	0.93	0.94	0.95
Total		0.93	0.94	0.94
n-9 polyunsaturated fatty acid				
Mead acid	20:3 n-9	1.03	1.03	1.02
n-6 /n-3 ratio		1.03	1.02	1.03

95% confidence intervals are shown when odds ratios are statistically significant or show a tendency toward significance.

[†] $p < 0.10$.* $p < 0.05$; [†] $p < 0.10$.** $p < 0.01$ vs controls.^a Multivariable models adjusted for sex and age.^b Multivariable models adjusted for sex, age, obesity, smoking status, alcohol consumption, diabetes, and thyroid and liver disease.

consistent with previous epidemiological studies [16,17]. Obesity is known to be a risk factor for OPLL [18], and may therefore be a confounding factor in the relationship between palmitic acid and OPLL. At the same time, however, this could be due to type I error. Because we are analyzing 20 fatty acids, it is to be expected that one of these fatty acids is significantly associated with OPLL - in this case palmitic acid.

This exploratory study was conducted without sample size calculation, because no associated studies were ever conducted before and no effect size was reported before. The effect size, which was calculated as the difference in the means between two groups divided by their combined standard deviation, for MA and total n-3 PUFAs were 0.006 and 0.13, respectively. MA was neutral also from these calculations. As for total n-3 PUFAs, if we had conducted the study with about 1000 subjects in each group, we could have seen a significant difference in plasma.

There were several limitations to this study. First, participants were recruited from a single hospital and thus the study cohort is not representative of the Japanese OPLL population as a whole. Second, selection bias might exist because we only recruited controls from patients with cervical spondylosis and/or lumbar disc disease. Third, no information regarding dietary intake of fatty acids was available.

Overall, no significant associations were found between OPLL risk and MA and n-3 PUFA levels. Palmitic acid did show a tendency toward a positive association with OPLL risk, however, this could be by chance. The biological significance of these fatty

acids requires further investigation. In the case of MA, it might be interesting to examine the relationship between its plasma (or more appropriately local tissue) concentration and the various clinical orthopedic conditions such as fracture healing and ectopic bone formation disease.

Author contributors

K. Hamazaki had full access to all data in the study and takes responsibility for the integrity of the data and accuracy of the data analysis.

Study concept and design: K. Hamazaki, Y. Kawaguchi, T. Hamazaki

Acquisition of data: K. Hamazaki, Y. Kawaguchi

Analysis and interpretation of data: K. Hamazaki, Y. Kawaguchi

Drafting of the manuscript: K. Hamazaki, Y. Kawaguchi

Critical revision of the manuscript for important intellectual content: K. Hamazaki, Y. Kawaguchi, M. Nakano, T. Yasuda, S. Seki, T. Hori, T. Hamazaki, T. Kimura

Statistical analysis: K. Hamazaki, Y. Kawaguchi

Obtained funding: Y. Kawaguchi

Administrative, technical, or material support: K. Hamazaki, Y. Kawaguchi

Study supervision: K. Hamazaki, Y. Kawaguchi

Table 4
Odds ratios and 95% confidence intervals for OPLL according to individual fatty acids.

	Fatty acid quartile					p for trend
		1 (Low)	2	3	4 (High)	
Myristic acid	14:0					
Range		< 0.213	0.213–0.263	0.263–0.290	0.290 <	
Case		13	34	21	38	
Control		27	27	27	28	
Model 1 ^a		1.0	1.72 (0.91–3.25)	1.35 (0.67–2.69)	1.77 (0.94–3.33)	0.19
Model 2 ^b		1.0	1.75 (0.92–3.33)	1.39 (0.69–2.79)	1.88 (0.99–3.56)	0.13
Model 3 ^c		1.0	1.95 (0.99–3.86)	1.60 (0.77–3.31)	1.94 (0.98–3.87)	0.19
Palmitic acid	16:0					
Range		< 28.2	28.2–29.2	29.2–30.1	30.1 <	
Case		13	24	26	43	
Control		27	27	27	28	
Model 1 ^a		1.0	1.45 (0.74–2.84)	1.51 (0.78–2.94)	1.86 (1.00–3.47)	0.049
Model 2 ^b		1.0	1.44 (0.74–2.84)	1.52 (0.78–2.97)	1.90 (1.01–3.58)	0.048
Model 3 ^c		1.0	1.32 (0.66–2.63)	1.40 (0.70–2.77)	1.75 (0.90–3.39)	0.091
Mead acid	20:3n-9					
Range		< 0.0516	0.0516–0.0732	0.0732–0.114	0.114 <	
Case		30	19	28	29	
Control		27	27	27	28	
Model 1 ^a		1.0	0.78 (0.44–1.39)	0.97 (0.58–1.62)	0.97 (0.58–1.61)	0.95
Model 2 ^b		1.0	0.77 (0.43–1.37)	0.97 (0.58–1.64)	0.94 (0.56–1.59)	1.00
Model 3 ^c		1.0	0.83 (0.46–1.49)	0.98 (0.57–1.67)	0.91 (0.53–1.57)	0.85
Eicosapentaenoic acid	20:5 n-3					
Range		< 1.73	1.73–2.48	2.48–3.93	3.93 <	
Case		28	24	33	21	
Control		27	27	27	28	
Model 1 ^a		1.0	0.92 (0.54–1.59)	1.08 (0.65–1.79)	0.84 (0.48–1.48)	0.74
Model 2 ^b		1.0	0.92 (0.53–1.58)	1.09 (0.65–1.83)	0.84 (0.47–1.51)	0.76
Model 3 ^c		1.0	0.87 (0.49–1.54)	1.07 (0.63–1.81)	0.82 (0.45–1.51)	0.76
Docosahexaenoic acid	22:6 n-3					
Range		< 6.07	6.07–7.16	7.16–8.16	8.16 <	
Case		30	25	27	24	
Control		27	27	27	28	
Model 1 ^a		1.0	0.91 (0.54–1.55)	0.95 (0.56–1.60)	0.88 (0.51–1.50)	0.68
Model 2 ^b		1.0	0.94 (0.54–1.61)	0.96 (0.56–1.65)	0.91 (0.52–1.60)	0.78
Model 3 ^c		1.0	0.99 (0.56–1.73)	0.88 (0.50–1.55)	0.92 (0.52–1.64)	0.70

^a Crude data.

^b Multivariable models adjusted for sex and age.

^c Multivariable models adjusted for sex, age, obesity, smoking status, alcohol consumption, thyroid disease, liver, renal disease, and diabetes.

Role of funding source

This work was partially supported by Grants-in-Aid for Scientific Research (#22591628, 2010–2012) from Japanese Ministry of Education, Culture, Sports, Science and Technology. Funds from the Investigation Committee on the Ossification of the Spinal Ligaments of the Japanese Ministry of Health, Labour and Welfare were also received, in part, to support this work. No relevant financial activities outside the submitted work. The funding source had no role in the study design; the collection, analysis, and interpretation of data; writing the report; or the decision to submit the paper for publication.

Acknowledgements

We are grateful to Ms. Shizuko Takebe (University of Toyama) for technical assistance.

References

[1] T. H. On an autopsied case of compression myelopathy with a callus formation in the cervical spinal canal, *Nihon-Geka-Hokan* 29 (1960) 1003–1007.

- [2] Y. Onji, H. Akiyama, Y. Shimomura, K. Ono, S. Hukuda, S. Mizuno, Posterior paravertebral ossification causing cervical myelopathy. A report of eighteen cases, *J. Bone Joint Surg. Am.* 49 (1967) 1314–1328.
- [3] N.E. Epstein, The surgical management of ossification of the posterior longitudinal ligament in 43 north americans, *Spine (Phila Pa 1976)* 19 (1994) 664–672.
- [4] N.E. Epstein, Ossification of the yellow ligament and spondylosis and/or ossification of the posterior longitudinal ligament of the thoracic and lumbar spine, *J. Spinal Disord.* 12 (1999) 250–256.
- [5] T. Sakou, E. Taketomi, S. Matsunaga, M. Yamaguchi, S. Sonoda, S. Yashiki, Genetic study of ossification of the posterior longitudinal ligament in the cervical spine with human leukocyte antigen haplotype, *Spine (Phila Pa 1976)* 16 (1991) 1249–1252.
- [6] J.F. Mead, W.H. Slaton Jr., Metabolism of essential fatty acids. III. Isolation of 5,8,11-eicosatrienoic acid from fat-deficient rats, *J. Biol. Chem.* 219 (1956) 705–709.
- [7] H.D.E. Adkisson, F.S. Risener Jr., P.P. Zarrinkar, M.D. Walla, W.W. Christie, R.E. Wuthier, Unique fatty acid composition of normal cartilage: discovery of high levels of n-9 eicosatrienoic acid and low levels of n-6 polyunsaturated fatty acids, *FASEB J.* 5 (1991) 344–353.
- [8] T. Hamazaki, N. Suzuki, R. Widyowati, et al., The depressive effects of 5,8,11-eicosatrienoic Acid (20:3n-9) on osteoblasts, *Lipids* 44 (2009) 97–102.
- [9] C.F. Dilling, A.M. Wada, Z.W. Lazard, et al., Vessel formation is induced prior to the appearance of cartilage in BMP-2-mediated heterotopic ossification, *J. Bone Miner. Res.* 25 (2010) 1147–1156.
- [10] T. Hamazaki, T. Nagasawa, K. Hamazaki, M. Itomura, Inhibitory effect of 5,8,11-eicosatrienoic acid on angiogenesis, *Prostaglandins Leukot Essent Fatty Acids* 86 (2012) 221–224.

Please cite this article as: K. Hamazaki, et al., Mead acid (20:3n-9) and n-3 polyunsaturated fatty acids are not associated with risk of posterior longitudinal ligament..., *Prostaglandins Leukotrienes Essent. Fatty Acids* (2015), <http://dx.doi.org/10.1016/j.plefa.2015.01.003>

- [11] Y.S. Chyun, L.G. Raisz, Stimulation of bone formation by prostaglandin E₂. Prostaglandins 27 (1984) 97–103.
- [12] Y. Ishida, S. Kawai, Characterization of cultured cells derived from ossification of the posterior longitudinal ligament of the spine, Bone 14 (1993) 85–91.
- [13] L. Wang, M.J. Huang, B. Liu, et al., Could heterotopic ossification be prevented by varying dietary n-3/n-6 polyunsaturated fatty acid ratio: a novel perspective to its treatment? Med. Hypotheses 80 (2013) 57–60.
- [14] E.G. Bligh, W.J. Dyer, A rapid method of total lipid extraction and purification, Can. J. Biochem. Physiol. 37 (1959) 911–917.
- [15] M. Itomura, S. Fujioka, K. Hamazaki, et al., Factors influencing EPA+DHA levels in red blood cells in Japan, In Vivo 22 (2008) 131–135.
- [16] D.A. Pan, S. Lillioja, M.R. Milner, et al., Skeletal muscle membrane lipid composition is related to adiposity and insulin action, J. Clin. Invest. 96 (1995) 2802–2808.
- [17] J.S. Perona, E. Gonzalez-Jimenez, M.J. Aguilar-Cordero, A. Sureda, F. Barcelo, Structural and compositional changes in erythrocyte membrane of obese compared to normal-weight adolescents, J. Membr. Biol. 246 (2013) 939–947.
- [18] W.R. Stetler, F. La Marca, P. Park, The genetics of ossification of the posterior longitudinal ligament, Neurosurg. Focus 30 (2011) E7.